ISSN 1070-3284, Russian Journal of Coordination Chemistry, 2022, Vol. 48, No. 5, pp. 261–269. © Pleiades Publishing, Ltd., 2022.
Russian Text © The Author(s), 2022, published in Koordinatsionnaya Khimiya, 2022, Vol. 48, No. 5, pp. 259–268.

Synthesis, Structures, and Properties of the Zn(II), Cu(II), Co(II), and Ni(II) Bis(chelate) Complexes Based on 2,4,9,11-Tetra-*tert*-butylbenzo[5,6][1,4]oxazino[2,3-*b*]phenoxazin-1-ol

M. G. Chegerev[a], *, O. P. Demidov[b], P. A. Knyazev[a], N. I. Makarova[a], A. G. Starikov[a], E. P. Ivakhnenko[a], and V. I. Minkin[a]

[a] *Institute of Physical and Organic Chemistry, Southern Federal University, Rostov-on-Don, Russia*
[b] *North Caucasus Federal University, Stavropol, Russia*
**e-mail: mchegerev@sfedu.ru*

Received October 12, 2021; revised October 21, 2021; accepted October 24, 2021

Abstract—A series of zinc, copper, cobalt, and nickel bis(chelate) complexes (**I**–**IV**) with 2,4,9,11-tetra-*tert*-butylbenzo[5,6][1,4]oxazino[2,3-*b*]phenoxazin-1-ol (LH) of the general formula ML_2 is synthesized. The spatial and electronic structures of the synthesized coordination compounds are studied by the density functional theory (DFT B3LYP/6-311++g(d,p)). The molecular structure of the adduct of the copper complex with pyridine (**II**·Py) is determined by X-ray diffraction (CIF file CCDC no. 2113818). The spectral characteristics of the ligand and related complexes are studied.

Keywords: heteropentacenes, chelate complexes, transition metals, density functional theory
DOI: 10.1134/S1070328422050037

INTRODUCTION

Search for new efficient luminophores and studies of energy transformation processes in the area of organic light emitting diodes (OLED) are urgent tasks of the modern chemistry and materials science [1–5]. The complexes of the main group metals with the ligands of the oxyquinoline type find wide use as photo- and electroluminescent materials [6–8]. Chelate tris(8-oxyquinoline)aluminum and bis(8-oxyquinoline)zinc capable of acting as emitting and electron transporting properties can be distinguished among the most frequently used complexes for the preparation of organic electronic devices [9–13].

The 4-hydroxyacridine and 1-hydroxyphenazine derivatives bearing the chelate fragment of hydroxyquinoline and π-expanded aromatic system are structural analogs of oxyquinolines. The structures and luminescence properties of the metal complexes based on similar ligands were described [14–19]. The modification of the considered above ligand systems by the introduction of additional heteroatoms (O or N) into the carbon skeleton results in the class of redox-active phenoxazines. A number of works devoted to studies of the structures and properties of the metal (both transition and nontransition) complexes based on phenoxazines in various redox states (neutral and ion-radical) has been published to date [20–31]. Phenomena of reversible electron transfer between the metal and ligand and exchange interactions between paramagnetic centers of diverse nature were found in the studied systems.

In the recent years chemists gave significant attention to substituted triphenodioxazines (TPDO) [32, 33], which are promising materials for the use in field transistors [34–36] and luminescent materials [37] and as dyes for the production of efficient solar cells [38, 39]. Similar compounds are structural analogs of pentacenes. However, unlike pentacenes, their structural analogs contain heteroatoms (O, N, S) in the carbon skeleton, which makes it possible to prepare ligand systems with finely tunable electronic and structural properties [40].

This work is devoted to the synthesis of new Zn(II), Cu(II), Co(II), and Ni(II) complexes based on sterically hindered 2,4,9,11-tetra-*tert*-butylbenzo-[5,6]-[1,4]oxazino[2,3-*b*]phenoxazin-1-ol (LH) and study of the physicochemical properties of the synthesized compounds. Ligand LH is heteropentacene containing the O,N-oxyquinoline fragment due to which chelate metal complexes can be formed. The study of a similar class of compounds would make it possible to extend concepts on the spatial and electronic structures of the complexes bearing chelate heteropentacene ligands.

EXPERIMENTAL

Perchlorate salts of the metals used in the works are commercially available. Ligand LH was prepared according to a known procedure [33]. The solvents used were purified and dehydrated using standard procedures.

Elemental analysis was carried out on an Elementar Vario El cube analyzer. EPR spectra were recorded on a Bruker EMX Plus spectrometer. 2,2-Diphenyl-1-picrylhydrazyl (g_i = 2.0037) was used as the standard for the determination of the *g* factor. EPR spectra were simulated using the Easyspin program package for Matlab [41]. Electronic absorption spectra were recorded for 2×10^{-5} M solutions on an Agilent 8453 spectrophotometer equipped with a temperature-maintained cell. All spectra were recorded in a standard 1-cm quartz cell at room temperature. Fluorescence measurements were carried out on a Cary Eclipse spectrofluorimeter (Varian). Dichloromethane (spectral purity grade, Acros Organics) was used to prepare solutions. IR spectra were recorded on a Varian Excalibur 3100 FTIR spectrometer.

Synthesis of ZnL_2 (I). A minor amount of Et_3N (0.1 mL) was added to a suspension of the ligand (0.05 g, 0.095 mmol) in THF (10 mL), and $Zn(ClO_4)_2 \cdot 6H_2O$ (0.017 g, 0.047 mmol) was added to the resulting mixture. The obtained reaction mixture was heated in a water bath (70°C) for 1 h. The reaction mixture changed color from red to intensive blue-violet. A finely dispersed powder precipitated after ethanol (10 mL) was added to the reaction mixture. The precipitate was filtered off in air and washed with small portions of ethanol and distilled water. The yield of a dark violet powder of complex **I** was 81%.

For $C_{68}H_{82}N_4O_6Zn$

Anal. calcd., %	C, 73.13	H, 7.40	N, 5.02
Found, %	C, 73.21	H, 7.33	N, 5.07

^{1}H NMR (THF-d_8; 20°C; δ, ppm): 7.33 (d, 1H, 2.3, H_{aryl}); 7.29 (d, 1H, 2.3, H_{aryl}); 7.17 (s, 1H, H_{aryl}); 6.89 (s, 1H, H_{aryl}); 6.59 (s, 1H, H_{aryl}); 1.34 (s, 9H, *t*-Bu); 1.40 (s, 9H, *t*-Bu); 1.49 (s, 9H, *t*-Bu); 1.46 (s, 9H, *t*-Bu).

IR (ν, cm^{-1}): 637 s, 725 m, 755 w, 781 w, 808 w, 851 m, 879 w, 915 m, 994 w, 1008 w, 1033 w, 1081 s, 1164 s, 1193 m, 1217 m, 1234 m, 1255 m, 1281 m, 1359 m, 1380 m, 1401 m, 1445 w, 1467 m, 1539 s, 1557 m, 1598 m, 1634 w, 2867 m, 2904 m, 2950 m.

Synthesis of CuL_2 (II) was carried out according to an analogous procedure using $Cu(ClO_4)_2 \cdot 6H_2O$ (0.017 g, 0.047 mmol) as the copper(II) ion source. The yield was 79%.

For $C_{68}H_{82}N_4O_6Cu$

Anal. calcd., %	C, 73.25	H, 7.41	N, 5.03
Found, %	C, 74.35	H, 7.30	N, 5.11

IR (ν, cm^{-1}): 638 s, 725 m, 756 w, 780 w, 808 w, 851 m, 878 w, 915 m, 995 w, 1008 w, 1031 w, 1081 s, 1163 s, 1193 m, 1219 m, 1234 m, 1257 m, 1280 m, 1357 m, 1379 m, 1402 m, 1444 w, 1466 m, 1538 s, 1559 m, 1598 m, 1633 w, 2867 m, 2906 m, 2950 m.

Synthesis of CoL_2 (III) was carried out according to an analogous procedure using $Co(ClO_4)_2 \cdot 6H_2O$ (0.017 g, 0.047 mmol) as the cobalt(II) ion source. The yield was 75%.

For $C_{68}H_{82}N_4O_6Co$

Anal. calcd., %	C, 73.56	H, 7.44	N, 5.05
Found, %	C, 73.44	H, 7.50	N, 5.10

IR (ν, cm^{-1}): 636 s, 724 m, 754 w, 780 w, 809 w, 851 m, 878 w, 916 m, 995 w, 1009 w, 1031 w, 1080 s, 1162 s, 1193 m, 1218 m, 1235 m, 1258 m, 1280 m, 1357 m, 1377 m, 1403 m, 1442 w, 1465 m, 1538 s, 1559 m, 1599 m, 1633 w, 2866 m, 2905 m, 2951 m.

Synthesis of NiL_2 (IV) was carried out according to an analogous procedure using $Ni(ClO_4)_2 \cdot 6H_2O$ (0.017 g, 0.047 mmol) as the nickel(II) ion source. The yield was 84%.

For $C_{68}H_{82}N_4O_6Ni$

Anal. calcd., %	C, 73.57	H, 7.45	N, 5.05
Found, %	C, 73.43	H, 7.51	N, 5.12

IR (ν, cm^{-1}): 634 s, 723 m, 754 w, 780 w, 810 w, 851 m, 878 w, 912 m, 998 w, 1009 w, 1034 w, 1082 s, 1162 s, 1193 m, 1215 m, 1235 m, 1259 m, 1280 m, 1356 m, 1377 m, 1402 m, 1442 w, 1464 m, 1538 s, 1558 m, 1597 m, 1633 w, 2867 m, 2902 m, 2950 m.

Quantum chemical calculations were performed using the Gaussian 16 program package [42] by the density functional theory (DFT) with the B3LYP functional [43] and 6-311++g(d,p) basis set for all atoms. The solvent (CH_2Cl_2) effects were taken into account using the CPCM model [44].

XRD of adduct **II**·Py was carried out at 293 K on an Agilent SuperNova diffractometer using the microfocus X-ray radiation source with the Cu anode and an Atlas S2 coordinate CCD detector. Reflections were collected and unit cell parameters were determined and refined using the CrysAlisPro 171.41.93a specialized software [45]. The structures were solved using the ShelXT program [46] and refined using the ShelXL program [47].

Compound **II**·Py crystallizes in the space group $I2/a$ ($a = 23.1152(3)$, $b = 9.63830(10)$, $c = 31.4930(4)$ Å, $\alpha = 90°$, $\beta = 111.0930(10)°$, $\gamma = 90°$, $V = 6546.25(14)$ Å^3, $Z = 4$, $\rho_{calc} = 1.212$ g/cm^3, $\mu = 0.903$ mm^{-1}). The number of measured reflections was 35698, and 6819 independent reflections ($R_{int} = 0.0238$) were used for structure determination and subsequent refinement of 397 parameters by full-matrix least squares in the anisotropic approximation for non-hydrogen atoms. The hydrogen atoms in **II**·Py were placed in the geometrically calculated positions and refined isotropically with the fixed thermal parameters $U(H)_{iso} = 1.2U(C)_{equiv}$ ($U(H)_{iso} = 1.5U(C)_{equiv}$ for methyl groups). After the final refinement, $wR_2 = 0.1244$ and $S(F^2) = 1.054$ for all reflections ($R_1 = 0.0402$ for all reflections that satisfy the condition $I > 2\sigma(I)$). The residual electron density maximum and minimum were 0.34/–0.25 e Å^{-3}.

The structure of adduct **II**·Py was deposited with the Cambridge Crystallographic Data Centre (CIF file CCDC no. 2113818; ccdc.cam.ac.uk/structures/).

RESULTS AND DISCUSSION

The main procedure for the synthesis of bis(chelate) complexes ZnL_2 (**I**), CuL_2 (**II**), CoL_2 (**III**), and NiL_2 (**IV**) with 2,4,9,11-tetra-*tert*-butylbenzo[5,6]-[1,4]oxazino[2,3-*b*]phenoxazin-1-ol (LH) is the reaction of perchlorate salts of the corresponding metals with the ligand in a ratio of 1 : 2 in THF. The deprotonating agent was Et_3N. Since the presented heteropentacene ligand is potentially redox-active, the synthesis was carried out using a vacuum line in order to exclude the influence of air oxygen on the reaction mechanism and products. Reflux of the reaction mixtures for 1 h results in a change in the color of the solutions from red to blue-violet. The addition of a minor amount of ethanol leads to precipitation. Complexes **I**–**IV** were isolated by filtration in air as dark violet powders in high yields (~80%). The synthesized compounds are resistant to air oxygen and moisture (Scheme 1).

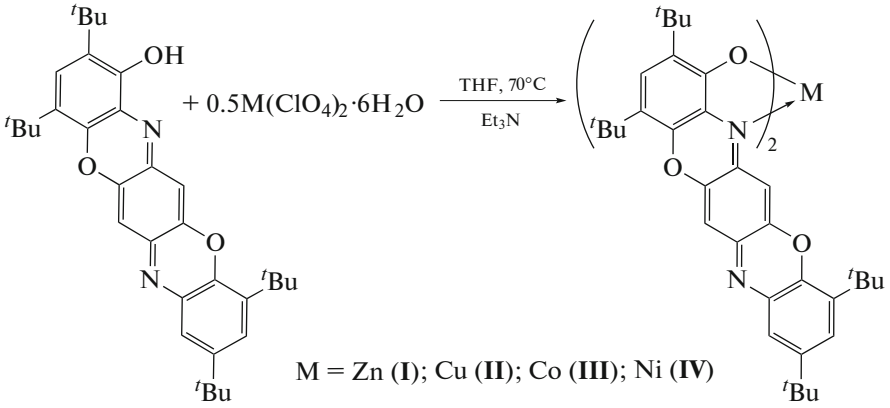

Scheme 1.

The synthesis using metal acetates with LH in a ratio of 1 : 2 in isopropyl alcohol in air was considered as an alternative procedure for the preparation of the complexes. The reaction mixture was refluxed in air for 1 h. The color changed from red to blue-violet. This approach leads to the formation of identical compounds **I**–**IV** but are characterized by lower yields of the final products (~65%).

The ^{1}H NMR spectrum measured in THF-d_8 is characterized by one set of signals of the coordinated ligand, indicating that the chelate ligands in the synthesized complex are equivalent. The signals from five protons at the aromatic rings range from 7.33 to 6.59 ppm, whereas the signals from the protons of four *tert*-butyl substituents appear in a characteristic range of 1.46–1.34 ppm.

All studied complexes showed a weak tendency to single crystal formation. However, needle-like single crystals suitable for XRD were isolated upon the slow evaporation of a solution of complex **II** in a toluene–pyridine (1 : 1) mixture for 1 month. The molecular structure of adduct **II**·Py is shown in Fig. 1. According to the XRD data, complex **II** reacts with a pyridine molecule to form pentacoordinated adduct **II**·Py. The coordination environment of the copper ion is a trigonal bipyramid with the N atoms of two O,N-chelate ligands and pyridine molecule in the base, whereas the apical positions are occupied by the oxygen atoms. The geometric parameter τ_5 is used to examine the coordination sphere of pentacoordinated complexes. In the case of an ideal square pyramid, $\tau_5 = 0$. In the case of an ideal trigonal bipyramid, $\tau_5 = 1$ [48]. The value $\tau_5 = 0.71$ calculated for compound **II**·Py corresponds to the tetragonal-distorted trigonal bipyramidal environment of the copper ion.

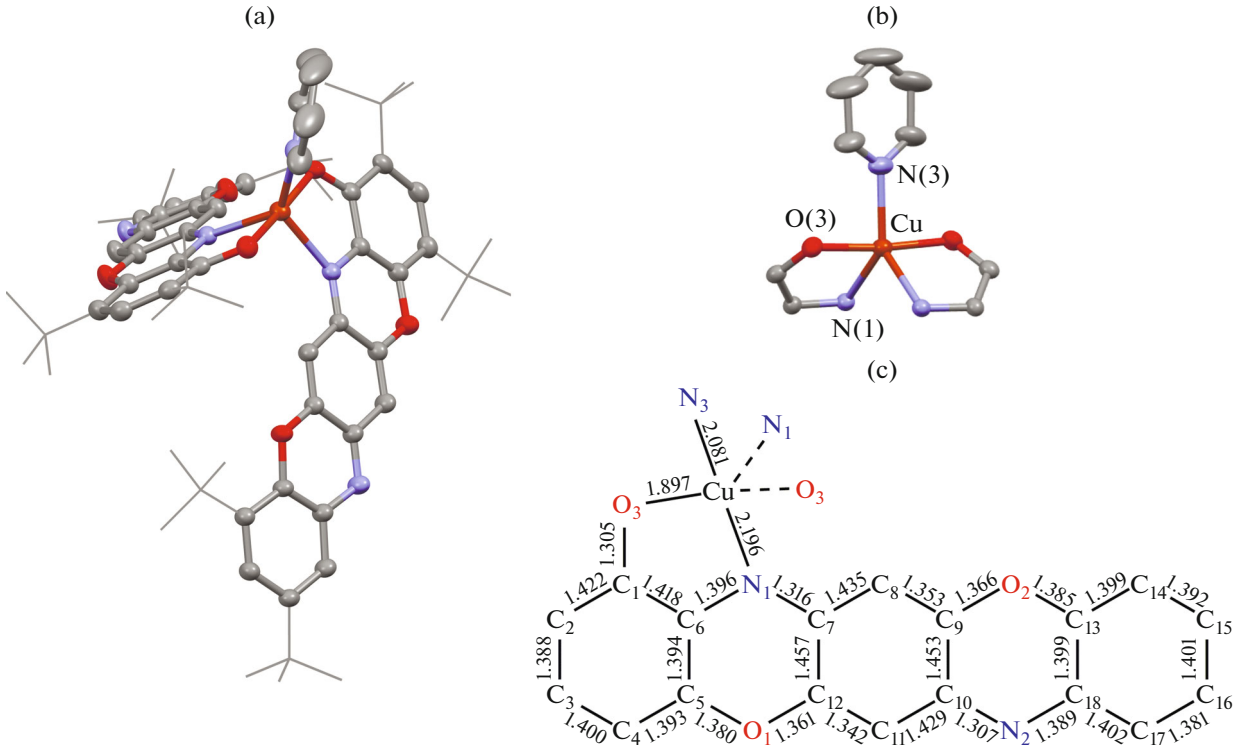

Fig. 1. (a) Molecular structure of adduct **II**·Py, (b) fragment of the coordination environment of the copper(II) ion, and (c) interatomic distances in the pentacyclic ligand (Å). Thermal ellipsoids for the key atoms are given with 50% probability. Hydrogen atoms are omitted for clarity.

Intermolecular interactions of various nature are observed in the crystal packing of adduct **II**·Py: CH···arene (~2.8 Å) and π–π-stacking interactions (3.3–3.9 Å) between the conjugated systems of the heteropentacene ligands of the adjacent molecules.

The Cu–O(3) (1.897 Å) and Cu–N(1) (2.196 Å) bond lengths lie in the range characteristic of the close in structure O,N-chelate copper complexes [48–51]. The distance between the copper atom and nitrogen atom (N(3)) of the coordinated pyridine molecule is 2.081 Å. Both pentacyclic ligands are identical in structure and structural parameters. The C(1)–C(6) and C(13)–C(18) bond lengths in the six-membered rings containing *tert*-butyl substituents are close to aromatic (1.40 Å), whereas the central moiety of the pentacyclic ligand exhibits a considerable quinoid distortion characterized by an alternation of the long and short C–C bonds (Fig. 1). The C(6)–N(1) (1.396(2) Å) and C(18)–N(2) (1.389(2) Å) distances are characteristic of ordinary carbon–nitrogen bonds, whereas C(7)–N(1) (1.316(2) Å) and C(10)–N(2) (1.307(2) Å) are appreciably shorter, indicating their multiple (C=N) nature. Thus, the available structural data suggest that in adduct **II**·Py the pentacyclic ligands exist in the monoanionic diamagnetic state.

This conclusion is satisfactorily consistent with the quantum chemical calculation results. The optimized geometry (DFT/B3LYP/6-311++g(d,p)) of adduct **II**·Py is characterized by the slightly elongated Cu–O and Cu–N bonds and demonstrates a noticeable tetragonal pyramidal distortion of the coordination polyhedron. This is due to the fact that crystal packing effects are ignored in the geometry optimization of a single molecule. The absence of a spin density (q_s) on the atoms of the conjugated system of the ligand confirms the conclusion about its monoanionic nature, whereas one lone electron is delocalized between the divalent copper ion (q_s^{Cu} = 0.60) and donor N (Σq_s = 0.21) and O (Σq_s = 0.19) atoms.

The geometry optimization of tetracoordinated complexes **I**–**IV** (DFT/B3LYP/6-311++g(d,p)) was performed in order to determine the molecular and electronic structures. According to the calculations, the coordination environment of the central metal ion in complexes **I**–**IV** composed of the O and N atoms of the chelating ligand is intermediate between planar square and tetrahedral environments. The geometric parameter τ_4, which is equal to zero in the case of the planar square geometry and to unity for the tetrahedral geometry, was used for the quantitative characterization of the polyhedron [51]. The structure of complex **II** is presented as an example in Fig. 2. The value of τ_4 calculated for complex **II** was 0.35, which allows one to describe the geometry of the complex as tetrahedral-distorted planar square. Selected metal–donor

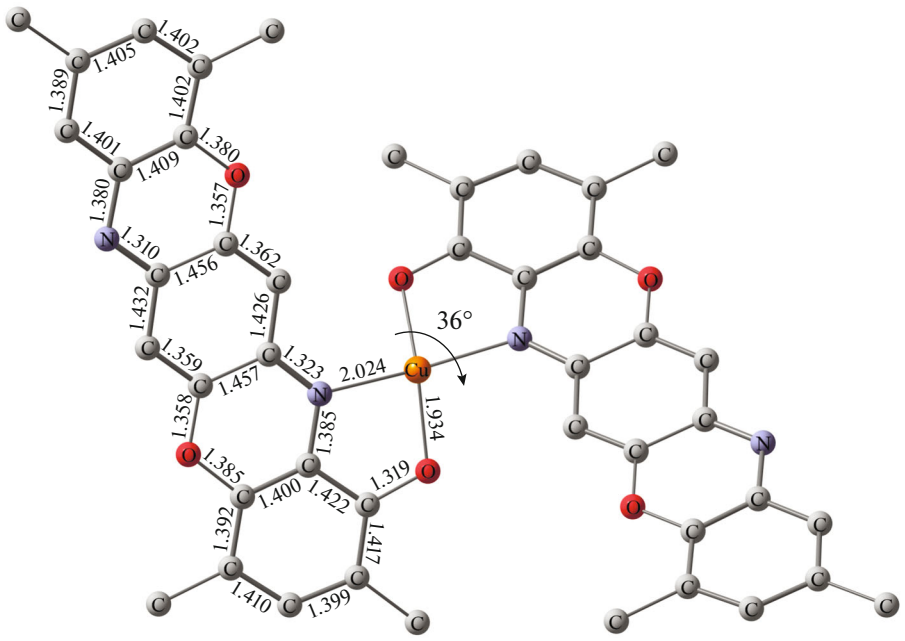

Fig. 2. Optimized geometry for complex **II** (DFT/B3LYP/6-311++g(d,p)). Bond lengths are given in Å. Hydrogen atoms and methyl substituents of the *tert*-butyl groups are omitted for clarity.

atom bond lengths for the series of compounds **I**–**IV** are listed in Table 1. The C–C and C–N bond lengths in the pentacyclic ligands are close to the values obtained earlier for adduct **II**·Py, indicating their monoanionic form. In spite of the potential redox activity of the pentacyclic ligand, the data obtained make it possible to describe the electronic structure of all the series of tetracoordinated complexes **I**–**IV** as follows: the divalent metal ion (M^{2+}) coordinated by two O,N-chelate monoanionic ligands (L^{-}). The spin density in complex **II**, like in adduct **II**·Py, is delocalized between the copper atom ($q_s^{Cu} = 0.58$) and donor atoms of the chelate unit ($\Sigma q_s = 0.41$).

Since cobalt(II) and nickel(II) ions capable of existing in both the low-spin (ls) and high-spin (hs) states are characterized by a high electron lability, possible isomers of complexes **III** and **IV** on the corresponding potential energy surfaces were studied. According to the calculations, the pseudotetrahedral high-spin ($S = 3/2$) state of complex **III** (hs-Co(II)) is the ground state, and the low-spin isomer ($S = 1/2$) containing ls-Co(II) is destabilized over the ground state by 12.5 kcal/mol. The latter is characterized by a significantly distorted (close to planar square) geometry of the coordination unit. The calculated value of q_s on the cobalt ion in the hs-Co(II) isomer of complex **III** is 2.705, which is somewhat lower than that expected for the free ion of high-spin cobalt(II) ($q_s^{Co} = 3$). This fact is due to the partial spin density delocalization between the donor oxygen and nitrogen atoms of the coordinated ligands.

A potential possibility of configurational isomerism, which is the reversible interconversion of the planar square isomer to the tetrahedral one, was predicted for the NiL_2 complex (**IV**) [52, 53]. According to the calculations, the ground state of compound **IV**,

Table 1. Selected bond lengths (Å) of complexes **I**–**IV** according to DFT B3LYP/6-311++g(d,p)

Complex	Bond (d, Å)		τ_4
	M–O	M–N	
I	1.943	2.082	0.76
II	1.934	2.024	0.35
III	1.936 (hs)	2.094 (hs)	0.72
	1.883 (ls)	1.988 (ls)	0.31
IV	1.923 (hs)	2.045 (hs)	0.71
	1.875 (ls)	1.926 (ls)	0.15

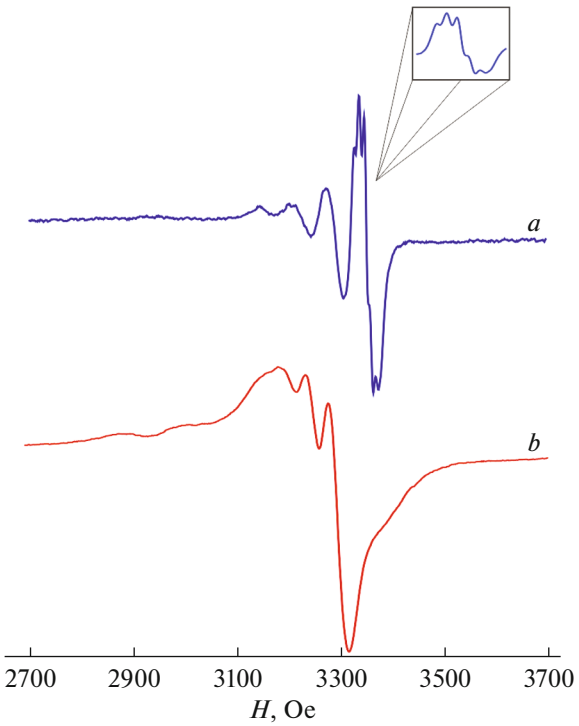

Fig. 3. EPR spectra of complex **II** in (a) toluene and (b) pyridine at 330 K.

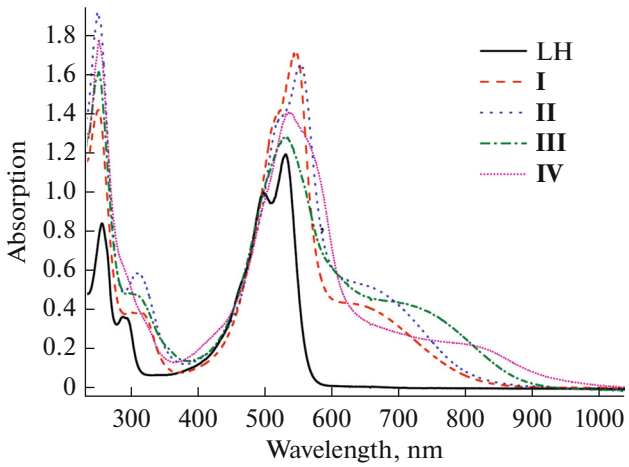

Fig. 4. Electronic absorption spectra of compounds LH and **I**–**IV** in dichloromethane at $T = 293$ K ($c = 2 \times 10^{-5}$ mol/L, $l = 1$ cm).

on the one hand, is the paramagnetic pseudotetrahedral isomer containing the divalent nickel ion in the high-spin state ($S = 1$). On the other hand, the diamagnetic planar square isomer ($S = 0$) is destabilized over the ground state by 3 kcal/mol only, indicating a high probability for configurational isomerism to occur. An analysis of the spin density distribution in the high-spin isomer showed a slightly underestimated value ($q_s^{Ni} = 1.618$) on the metal ion (hs-Ni(II)), which, like in compound **III**, is due to its partial delocalization in the chelate fragments.

The isotropic EPR spectrum was recorded for compound **II** ($S = 1/2$) in a toluene solution at 330 K (Fig. 3*a*) and demonstrates an anisotropically broadened quartet caused by the hyperfine coupling (HFC) of the lone electron with the magnetic copper isotopes (^{63,65}Cu, $I = 3/2$). This spectral shape is characteristic of a similar type of the tetracoordinated copper(II) complexes [49, 50, 54]. It should be mentioned that the most intense and high-field component of the spectrum demonstrates the hyperfine structure (HFS) caused by the HFC of the lone electron with two equivalent magnetic nuclei of the nitrogen atom (^{14}N, $I = 1$) of the coordinated chelate ligands. The experimentally determined values of HFC constants and g factor are as follows: $a_i(^{63,65}\text{Cu}) = 66.5$ Oe, $a_i(^{14}\text{N}) = 10$ Oe, and $g_i = 2.14$.

The replacement of the solvent by pyridine results in significant changes in the EPR spectrum of complex **II** (Fig. 3*b*) caused by an additional coordination of the pyridine molecule with the formation of adduct **II**·Py. This is accompanied by a considerable change in the geometry of the coordination polyhedron from the distorted planar square to trigonal pyramidal geometry. The HFC constant with ^{63,65}Cu is 140 Oe ($g_i = 2.24$). The available data suggest that the coordination of the pyridine molecule is accompanied by a change in the electronic structure of the central copper ion, which is shown by a considerable change in the shape and parameters of the EPR spectrum.

In order to study the influence of the metal nature on the spectral properties of coordination compounds **I**–**IV**, the optical and photoluminescence properties in a dichloromethane solution at room temperature were studied in comparison. The electronic absorption spectra of solutions of ligand LH and related complexes **I**–**IV** are shown in Fig. 4. The experimental data are systematized in Table 2.

The electronic absorption spectrum of ligand LH in a spectral range of 400–1000 nm is characterized by an intense structured absorption band with two maxima at 496 and 529 nm and molar absorption coefficients of 49900 and 59700 mol L^{-1} cm^{-1}, respectively (Table 2, Fig. 4). Time dependent DFT (TD-DFT) calculations were performed to establish the nature of the observed electron transitions and showed a good agreement with the experimental data. The calculated intense bands in a range of 490–530 nm correspond to π–π transitions between the highest occupied molecular orbital (HOMO) and lowest unoccupied molecular orbital (LUMO). The LUMO is mainly localized on the central *para*-quinone fragment of heteropentacene, whereas the HOMO is localized on the aromatic rings of the aminophenolate moieties of the ligand (Fig. 5).

Table 2. Spectral data for LH and complexes **I**–**IV** in dichloromethane at 293 K

Compound	Absorption λ_{max}, nm (ε, 10^3 mol L^{-1} cm^{-1})
LH	254 (41.9), 286 (18.1), 496 (49.9), 529 (59.7)
I	249 (71.0), 309 (19.2), 545 (85.8), 625 sh (21.6)
II	249 (96.3), 309 (29.2), 550 (82.5), 630 sh (26.9)
III	250 (80.8), 305 sh (23.7), 530 (64.2), 700 sh (21.6)
IV	250 (89.3), 287 sh (30.6), 536 (70.6), 800 sh (11.0)

Unlike ligand LH, the spectra of complexes **I**–**IV** exhibit a new absorption band with maxima in a range of 625–800 nm (ε = 11000–26900 mol L^{-1} cm^{-1}) along with the band at 530–550 nm (ε = 64200–85800 mol L^{-1} cm^{-1}) in the same spectral range (Table 2, Fig. 4). Complex formation results in a significant bathochromic shift of the long-wavelength absorption maxima of coordination compounds **I**–**IV** relative to the ligand by 96–271 nm, which is visually observed as deepening of the color of solutions of the complexes compared to solutions of the ligand that changed from orange to dark violet. According to the TD-DFT calculation results, the absorption band in the spectra of compounds **I**–**IV** in a range of 530–550 nm have the same nature as that observed for free ligand LH, whereas the new band in a range of 625–800 nm is due to the charge transfer from the O,N-chelate metallocycles of the molecule (HOMO) to the central *para*-quinone (LUMO) fragments of the ligands. The frontier orbitals of LH and complex **I**

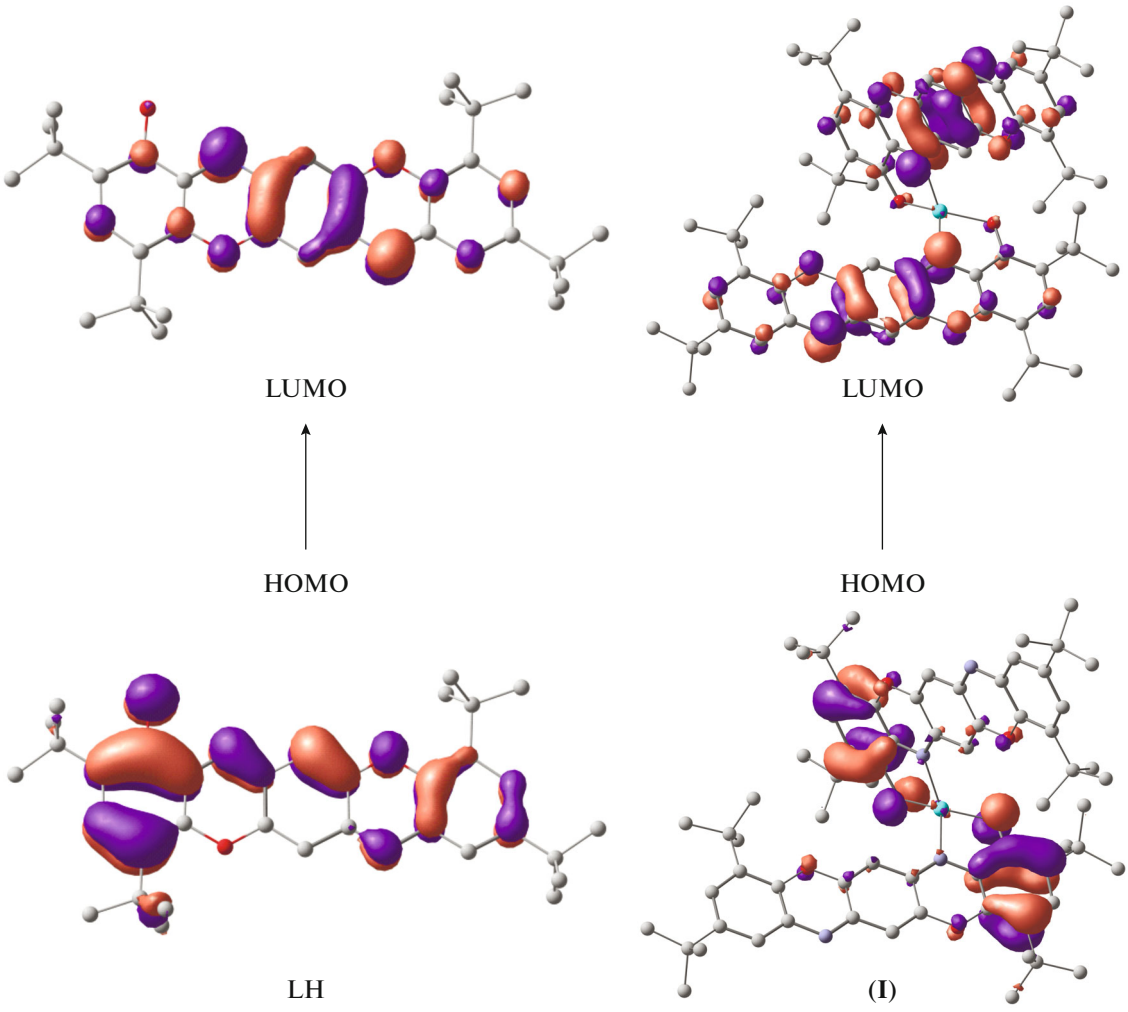

Fig. 5. Frontier orbitals of LH and complex **I** involved in the transitions at 500–530 and 625 nm, respectively.

involved in the discussed transitions are shown in Fig. 5.

An analysis of the spectral characteristics of the studied compounds shows that the zinc and copper complexes have nearly the same optical properties, which is confirmed by the absorption bands close in shape, position, and intensity (Table 2, Fig. 4). The bathochromic shift of the maxima of the long-wavelength absorption bands of complexes **I** and **II** compared to ligand LH is 96 and 101 nm, respectively. At the same time, the cobalt (**III**) and nickel (**IV**) complexes demonstrate a significant absorbance shift ($\Delta\lambda = 75–175$ nm) to the near-IR spectral range compared to the copper and zinc complexes.

It is known from the published data that the heteropentacene ligands close in structure to the ligand used in this work demonstrate intense fluorescence and are characterized by high photostability [33]. At the same time, the study of the photophysical properties of LH and related complexes **I**–**IV** showed that both the ligand and its complexes exhibited no appreciable photoluminescence properties in solutions at room temperature.

Thus, the series of the zinc, copper, cobalt, and nickel bis(chelate) complexes with 2,4,9,11-tetra-*tert*-butylbenzene[5,6][1,4]oxazino[2,3-*b*]phenoxazin-1-ol was synthesized. The geometric and electronic characteristics of the synthesized compounds were studied using the density functional theory. The tetracoordinated complexes are characterized by a distorted geometry of the coordination polyhedron, which is intermediate between the pseudotetrahedral and square planar geometries. The molecular structure of the pentacoordinated adduct of the copper complex with pyridine was determined by XRD. An analysis of the structural parameters indicates the diamagnetic monoanionic form of the heteropentacene ligand in all synthesized compounds. The optical properties of the ligand and synthesized complexes were studied.

FUNDING

This work was supported by the Russian Science Foundation, project no. 19-13-00022.

CONFLICT OF INTEREST

The authors declare that they have no conflicts of interest.

REFERENCES

1. Chen, C.H. and Shi, J., *Coord. Chem. Rev.*, 1998, vol. 171, p. 161.
2. Mitschke, U. and Bauerle, P., *J. Mater. Chem.*, 2000, vol. 10, p. 1471.
3. *Organic Light-Emitting Diodes (OLEDs): Materials, Devices and Applications*, Buckley, A., Ed., Philadelphia: Woodhead Publishing Limited, 2013.
4. *OLED Fundamentals: Materials, Devices, and Processing of Organic Light-Emitting Diodes*, Gaspar, D.J. and Polikarpov, E., Eds., Boca Raton: Taylor & Francis Group, 2015.
5. Bunzli, J.-C.G. and Piguet, C., *Chem. Soc. Rev.*, 2005, vol. 34, p. 1048.
6. Tsuboi, T., Nakai, Y., and Torii, Y., *Centr. Eur. J. Phys.*, 2012, vol. 10, p. 524.
7. Shen, L., Li, F.Y., Sha, Y.W., et al., *Tetrahedron Lett.*, 2004, vol. 45, p. 3961.
8. Monzon, L.M.A., Burke, F., and Coey, J.M.D., *J. Phys. Chem.*, 2011, vol. 115, p. 9182.
9. Hamada, Y., Sano, T., Fujita, M., et al., *Jpn. J. Appl. Phys. Pt 2*, 1993, vol. 32, p. L514.
10. Sapochk, L.S., Benincasa, F.E., Schofield, R.S., et al., *J. Am. Chem. Soc.*, 2002, vol. 124, p. 6119.
11. Dumur, F., *Synth. Met.*, 2014, vol. 195, p. 241.
12. Hopkins, T.A., Meerholz, K., Shaheen, S., et al., *Chem. Mater.*, 1996, vol. 8, p. 344.
13. Mishra, A., Nayak, P.K., and Periasamy, N., *Tetrahedron Lett.*, 2004, vol. 45, p. 6265.
14. Mastropietro, T.F., Szerb, E.I., Deda, M.L., et al., *Eur. J. Inorg. Chem.*, 2013, vol. 2013, p. 2188.
15. Balashova, T.V., Polyakova, S.K., Arsenyev, M.V., et al., *Eur. J. Inorg. Chem.*, 2021, p. 1441.
16. Balashova, T.V., Arsenyev, M.V., Polyakova, S.K., et al., *J. Mol. Struct.*, 2021, vol. 1229, p. 129798.
17. Miozzo, L., Papagni, A., Casalbore-Miceli, G., Del Buttero, P., et al., *Chem. Mater.*, 2004, vol. 16, p. 5124.
18. Aiello, I., Aiello, D., and Ghedini, M., *J. Coord. Chem.*, 2009, vol. 62, p. 3351.
19. Ukwitegetse, N., Femia, D., Sylvinson Muthiah Ravinson, D., et al., *Inorg. Chem.*, 2021, vol. 60, p. 866.
20. Stegmann, H.B. and Scheffler, K., *Chem. Ber.*, 1968, vol. 101, p. 262.
21. Whalen, A.M., Bhattacharya, S., and Pierpont, C.G., *Inorg. Chem.*, 1994, vol. 33, p. 347.
22. Speier, G., Whalen, A.M., Csihony, J., and Pierpont, C.G., *Inorg. Chem.*, 1995, vol. 34, p. 1355.
23. Ivakhnenko, E.P., Starikov, A.G., Minkin, V.I., et al., *Inorg. Chem.*, 2011, vol. 50, p. 7022.
24. Antipin, M.Yu., Ivakhnenko, E.P., Koshchienko, Yu.V., et al., *Russ. Chem. Bull.*, 2013, vol. 62, p. 1744.
25. Romanenko, G.V., Ivakhnenko, E.P., Minkin, V.I., et al., *Inorg. Chim. Acta*, 2014, vol. 418, p. 66.
26. Ivakhnenko, E.P., Starikov, A.G., Lyssenko, K.A., et al., *Inorg. Chim. Acta*, 2014, vol. 410, p. 144.
27. Ranis, L.G., Werellapatha, K., Pietrini, N.J., et al., *Inorg. Chem.*, 2014, vol. 53, p. 10203.
28. Ivakhnenko, E.P., Koshchienko, Yu.V., Knyazev, P.A., et al., *Russ. J. Coord. Chem.*, 2016, vol. 42, p. 509. https://doi.org/10.1134/S1070328416040011
29. Ivakhnenko, E.P., Romanenko, G.V., Simakov, V.I., et al., *Inorg. Chim. Acta*, 2017, vol. 458, p. 116.
30. Galley, S.S., Pattenaude, S.A., Gaggioli, C.A., et al., *J. Am. Chem. Soc.*, 2019, vol. 141, p. 2356.

31. Chegerev, M.G., Arsenyeva, K.V., Cherkasov, A.V., and Piskunov, A.V., *Russ. J. Coord. Chem.*, 2020, vol. 46, p. 746. https://doi.org/10.1134/S1070328420110019
32. Seidel, P., *Chem. Ber.*, 1890, vol. 23, p. 182.
33. Ivakhnenko, E.P., Romanenko, G.V., Makarova, N.I., et al., *Dyes Pigments*, 2020, vol. 176, p. 108174.
34. Chong-an, D., Li, J., Yu, G., et al., *Org. Lett.*, 2008, vol. 10, p. 3025.
35. Nicolas, Y., Castet, F., Devynck, M., et al., *Org. Electron.*, 2012, vol. 13, p. 1392.
36. Gruntz, G., Lee, H., Hirsch, L., et al., *Adv. Electron. Mater.*, 2015, p. 1500072.
37. Tanaka, T., Ashida, T., and Matsumoto, S., *Chem. Lett.*, 2011, vol. 40, p. 573.
38. Allama, N.Y., Lepeltier, F., Massin, M., et al., *Chem.-Eur. J.*, 2014, vol. 20, p. 3678.
39. Gong, X., Han, P., Wen, H., et al., *Eur. J. Org. Chem.*, 2017, p. 3689.
40. Miao, Q., *Synlett*, 2012, vol. 23, p. 326.
41. Stoll, S. and Schweiger, A.J., *J. Magn. Reson.*, 2006, vol. 178, p. 42.
42. Frisch, M.J., Trucks, G.W., Schlegel, H.B., et al., *Gaussian 16. Revision C. 01*, Wallingford: Gaussian, 2019.
43. Becke, A.D., *J. Chem. Phys.*, 1993, vol. 98, p. 5648.
44. Barone, V. and Cossi, M., *J. Phys. Chem. A*, 1998, vol. 102, p. 1995.
45. *CrysAlisPro. Version 171.41.93a*, Rigaku Oxford Diffraction, 2015. https://www.rigaku.com/products/crystallography/crysalis.
46. Sheldrick, G.M., *Acta Crystallogr., Sect. A: Found. Adv.*, 2015, vol. 71, p. 3.
47. Sheldrick, G.M., *Acta Crystallogr., Sect. C: Struct. Chem.*, 2015, vol. 71, p. 3.
48. Addison, A.W., Rao, T.N., Reedijk, J., et al., *Dalton Trans.*, 1984, p. 1349.
49. Lada, Z.G., Sanakis, Y., Raptopoulou, C.P., et al., *Dalton Trans.*, 2017, vol. 46, p. 8458.
50. Ivakhnenko, E.P., Knyazev, P.A., Vitkovskaya, Y.G., et al., *Eur. J. Inorg. Chem*, 2021, vol. 2021, p. 2055.
51. Yang, L., Powell, D.R., and Houser, R.P., *Dalton Trans.*, 2007, no. 9, p. 955.
52. Ernst, R.E., O'Connor, M.J., and Holm, R.H., *J. Am. Chem. Soc.*, 1967, vol. 89, p. 6104.
53. Garnovskii, A.D., Nivorozhkin, A.L., and Minkin, V.I., *Coord. Chem. Rev.*, 1993, vol. 126, p. 1.
54. Antholine, W.E., Bennett, B., and Hanson, G.R., in *Multifrequency Electron Paramagnetic Resonance*, Misra, S.K., Ed., Wiley-VCH, 2011, p. 647.

Translated by E. Yablonskaya